

## Chirality-Controlled Syntheses of Double-Helical Au Nanowires

Makoto Nakagawa, and Takeshi Kawai

*J. Am. Chem. Soc.*, **Just Accepted Manuscript** • DOI: 10.1021/jacs.8b00910 • Publication Date (Web): 03 Apr 2018

Downloaded from <http://pubs.acs.org> on April 3, 2018

### Just Accepted

“Just Accepted” manuscripts have been peer-reviewed and accepted for publication. They are posted online prior to technical editing, formatting for publication and author proofing. The American Chemical Society provides “Just Accepted” as a service to the research community to expedite the dissemination of scientific material as soon as possible after acceptance. “Just Accepted” manuscripts appear in full in PDF format accompanied by an HTML abstract. “Just Accepted” manuscripts have been fully peer reviewed, but should not be considered the official version of record. They are citable by the Digital Object Identifier (DOI®). “Just Accepted” is an optional service offered to authors. Therefore, the “Just Accepted” Web site may not include all articles that will be published in the journal. After a manuscript is technically edited and formatted, it will be removed from the “Just Accepted” Web site and published as an ASAP article. Note that technical editing may introduce minor changes to the manuscript text and/or graphics which could affect content, and all legal disclaimers and ethical guidelines that apply to the journal pertain. ACS cannot be held responsible for errors or consequences arising from the use of information contained in these “Just Accepted” manuscripts.

# Chirality-Controlled Syntheses of Double-Helical Au Nanowires

Makoto Nakagawa and Takeshi Kawai\*

Department of Industrial Chemistry, Tokyo University of Science, 1-3 Kagurazaka, Shinjuku-ku, Tokyo 162-8601, Japan

## Supporting Information Placeholder

**ABSTRACT:** The selective large-scale syntheses of noble metal nano-crystals with complex shapes using wet-chemical approaches remain exciting challenges. Here we report the chirality-controllable syntheses of double-helical Au nanowires (NWs) using chiral soft-templates composed of two organogelators with their own active functions; one organogelator serves to introduce helicity into the template and the other acts as a capping agent to control the Au shape. One-dimensional twisted-nanoribbon templates are prepared simply by mixing the two organogelators in water containing a small amount of toluene, followed by the addition of LiCl; template chirality is controlled through the selection of the handedness of the helicity-inducing organogelator. Double-helical Au NWs synthesized on these chiral templates have the same helical structure as the template because the Au NWs grow along both edges of the twisted nanoribbons with right- or left-handed helicities. Dispersions of the right- and left-handed double-helical Au NWs exhibit opposite CD signals.

Molecular chirality is a major topic in chemistry and biology because chirality is a key molecular-recognition concept.<sup>1</sup> In addition to organic chiral molecules, chiral metallic nanomaterials have recently attracted significant attention due to their unique chiroptical properties, such as large optical activities<sup>2</sup> and negative refractions<sup>3</sup> induced by plasmonic chirality. The key to realizing the desired chiroptical properties relies critically on the technique used to fabricate the chiral metallic nano-object.

Imparting chirality to the metallic nano-object is the most intuitive approach for introducing chiroptical properties. Two types of processes introduce chiral shapes to metallic nano-objects with controllable chirality. One is a physical-production process; for instance a mechanical-control process in which the metallic nano-object is fabricated using deposition or etching equipment that installs a rotational component mechanically.<sup>4</sup> For example, Fischer and colleagues<sup>4a</sup> fabricated left- and right-handed Au nanohelices by glancing-angle deposition onto a rotating substrate in clockwise and anticlockwise directions, and showed that these materials exhibit opposite CD spectra with distinct positive and negative Cotton effects. Physical processes are the most

straightforward for the fabrication of nano-objects and afford complicated chiral nanostructures with high precision, although there is significant room for improvement in productivity. The other is a chemical-production process that uses chiral nanostructures induced by chiral organic molecules.<sup>5-10</sup> This process can be applied to wet chemical syntheses using chiral templates such as the organic biomolecular scaffolds of DNA,<sup>5</sup> peptides,<sup>6</sup> and self-assembled amphiphiles.<sup>7</sup> This approach has produced helical arrays of achiral metal nanoparticles (NPs) deposited on chiral templates that exhibit strong chiroptical activities.<sup>7d</sup> For example, Rosi and colleagues<sup>6a</sup> fabricated a helical array of spherical Au NPs using left- and right-handed helical molecular aggregates composed of L- and D-peptide conjugates as templates. Although wet chemical synthesis is advantageous for preparing metal nano-objects on the large scale, there are very few reports of the fabrication of chiral metallic nano-objects by wet chemical methods<sup>10</sup> because most of the reported chiral templates do not introduce shape-controlled functionality to the metal NPs themselves. Consequently, the nano-objects produced using these approaches are essentially chiral arrays of achiral metal NPs.<sup>5-8</sup>

To fabricate chiral-shaped metal nanocrystals using chiral templates through wet chemical synthesis, the templates are required to possess two functional moieties; the first induces chirality into the template and the second controls the growth direction of the metal nanocrystals along the chiral template. The introduction of both functions into a single compound through molecular design and synthesis is challenging. Accordingly, we introduce a role-sharing strategy in this report; a template of chiral Au nanocrystals was constructed using two compounds; each compound provides the individual functions required for introducing chirality into the template and producing shape-controlled Au nanocrystals.

We report a chirality-controlled synthesis of ultrathin (average diameter ~3.0 nm) double-helical Au nanowires (NWs) using a chiral soft-template. The template was prepared using two kinds of organogelators and facilitates both soft-templating and the anisotropic growth of Au nanocrystals. Chiral D-12-hydroxystearic acid (D-HSA, Figure 1) was used as the organogelator that introduces chirality into the structure of the soft-template because D-HSA self-assembles to form ribbon-like nanostructures with a right-handed twist.<sup>11</sup>

D-HSA is a well-known organogelator used in commercial products, and enantiopure D-HSA is easily obtained in large quantities by the hydrogenation and hydrolysis of castor oil.<sup>12</sup> Furthermore, L-HSA (Figure 1), with the opposite chirality to D-HSA, forms left-handed twisted nanoribbons, and can be synthesized through the chiral inversion of D-HSA (Scheme S1).<sup>11</sup> A long chain amidoamine (C18AA, Figure 1) was selected as the other organogelator because C18AA affords a platform for the preparation of Au NWs due to its significant propensity to control the growth of metal crystals, which is ascribed to the selective adsorption properties the terminal amine groups of C18AA for particular crystal faces of gold.<sup>13</sup> We have already fabricated straight ultrathin Au NWs,<sup>13a</sup> dendritic Au NWs,<sup>13b</sup> and Pd NWs<sup>14</sup> assisted by the capping and soft-template functions of C18AA.

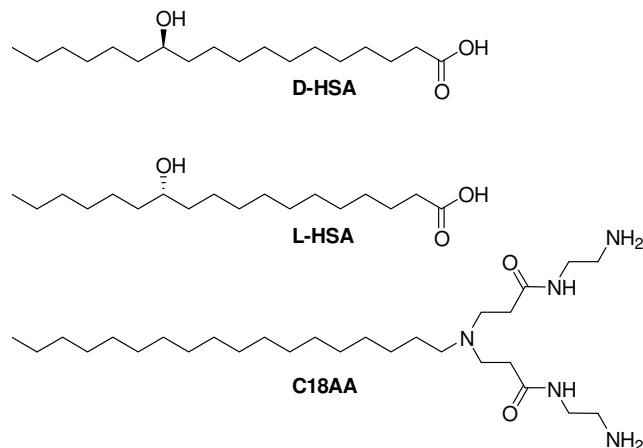


Figure 1. Chemical structures of D-HSA, L-HSA and C18AA.

Chiral soft-templates composed of D- or L-HSA, and C18AA were prepared as described in the Supporting Information (SI). In brief, D- or L-HSA, and C18AA (molar ratio = 1:6) were mixed in water with a small amount of toluene, followed by the addition of aqueous LiCl solution. The addition of LiCl is crucial and promotes the formation of semi-transparent hydrogels within 30 min at room temperature. It should be noted that a mixture of the water-soluble C18AA organogelator and water-insoluble HSA formed a hydrogel, whereas each organogelator separately does not form a hydrogel. Furthermore, the hydrogel exhibits a thermal reversible phase transition from gel to sol upon heating (Figure S5), indicating that the hydrogel is composed of a thermodynamically stable product.

Figures 2a and 2b show scanning electron microscopy (SEM) images of dried hydrogels prepared from D- and L-HSA, respectively; many twisted nanoribbons with homogenous structures are clearly visible. Both entangled nanoribbons are highly uniform with periodic sizes and shapes, and exhibit  $168 \pm 12$  nm (D-HSA) and  $171 \pm 9$  nm (L-HSA) helical pitches,  $26.9 \pm 3.1$  nm (D-HSA) and  $26.3 \pm 3.0$  nm (L-HSA) diameters, and  $12.1 \pm 0.9$  nm (D-HSA) and  $12.1 \pm 0.8$  nm (L-HSA) thicknesses, whereas they exhibit opposite helicities; the nanoribbons produced by the D- and L-HSA systems have right- and left-handed twist structures, respectively (Figures 2, S6 and S7). This result verifies that the handedness of the self-assembled twisted nanoribbon is completely controllable by the chirality of the HSA used as the chiral source.

The observation that the twisted nanoribbons are reversibly produced following thermal sol-gel phase-transition cycles,

and the apparent homogeneous structures depicted in Figures 2a and b, indicate that the nanoribbons have specific chemical compositions. The molar ratios of HSA to C18AA in the nanoribbons were determined to be 4:1 by <sup>1</sup>H-NMR spectroscopy of the filtered nanoribbons, although the ratio of the original preparation mixture was 1:6 (Figure S8). In other words, most of the water-soluble C18AA molecules remain in the bulk aqueous solution. Furthermore, twisted nanoribbons with the same structures and compositions were obtained using molar ratios that ranged from 1:12 to 1:4 in the preparation mixture (Figure S9).

From the nanoribbon thickness of 12.3 nm and the 1:4 molar ratio of C18AA to HSA, these nanoribbons are probably composed of one C18AA bilayer and two HSA bilayers, since bilayer thicknesses of 4.67<sup>15</sup> and 3.73 nm<sup>13a</sup> were reported for HSA and C18AA, respectively. Figures 2c and S10 show the proposed structures of the nanoribbons; the C18AA bilayer is sandwiched between two HSA bilayers, in which ionic bonds between the NH<sub>2</sub> groups of the C18AA and the COOH groups of the HSA are formed through acid/base interactions at the interface. Furthermore, the carboxyl groups on the outer sides of HSA probably bind lithium ions. The formation of a carboxylate band and the absence of a carboxylic acid band in the FT-IR spectrum of the hydrogel (Figure S11). Layers of lithium hydroxystearate on both outer sides of the nanoribbon may prevent the adsorption of additional C18AA layers. This proposal is consistent with the observation that large tabular crystals, instead of nanoribbons, are formed in the absence of LiCl (Figure S12).

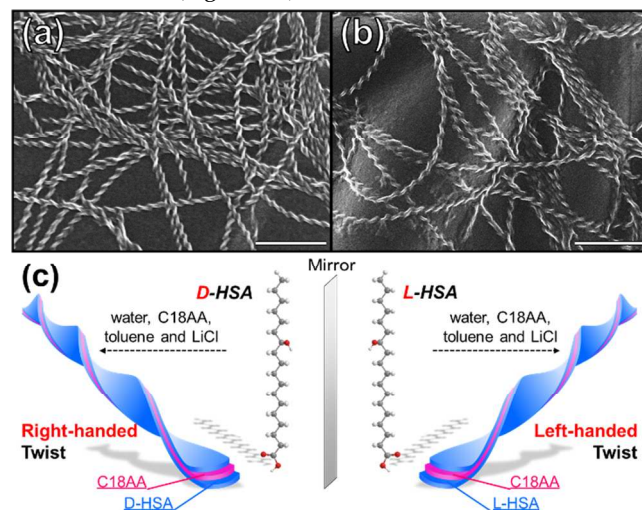


Figure 2. SEM images of twisted nanoribbons prepared using (a) D-HSA and (b) L-HSA. Scale: 500 nm. (c) Illustrating the preparation of twisted nanoribbons as soft-templates with controllable helicities.

As C18AA molecules that act as soft-templates for Au nanocrystal growth are exposed along both edges of each nanoribbon (Figure 2c), double-helical Au NWs can be grown along both edges. The Au NWs were synthesized by adding a solution of a gold precursor, a reducing agent, a pH adjusting agent and LiCl to the solution used to prepare the HSA/C18AA soft-template described above (see SI for details). Even in the presence of the gold precursor and the reducing agent, the mixture forms a hydrogel and produces the same nanoribbon described above (Figures 3e, S6, and

S7). The color of the mixture gradually changed from yellow to dark brown because of the formation of Au nanocrystals (Figure 3a and b). Figure 3c shows a transmission electron microscopy (TEM) image of the resultant Au-nanocrystalline products. Multiple meandering Au NWs with diameters of  $3.0 \pm 0.4$  nm (D-HSA) and  $3.0 \pm 0.5$  nm (L-HSA) are clearly visible, with few particulate byproducts (Figure S13). Interestingly, many of the meandering Au NWs exhibit double-helical structures with  $170 \pm 11$  (D-HSA) nm and  $168 \pm 9$  (L-HSA) nm helical pitches, and  $21.8 \pm 2.3$  nm (D-HSA) and  $21.8 \pm 2.0$  nm (L-HSA) widths (Figures S14 and S15). This observation clearly reveals that the morphology of the nanoribbon is transferred to that of the Au NW because the double-helical Au NWs have almost identical structures to those of the nanoribbons used as the soft-templates (Figures 3d, e, and S16). Note that there were sometimes two nanowires at one edge of the nanoribbons (Figure 3c). This is probably due to the fact that there are two boundaries between HSA and C18AA in the nanoribbons, which can be used as the adsorption sites of Au (Figure S10).

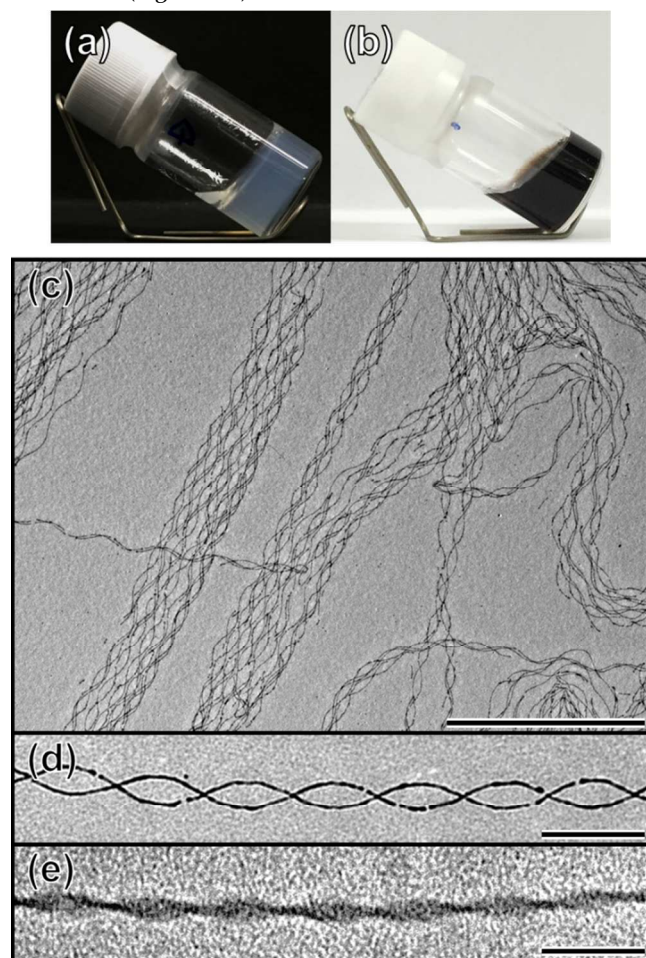


Figure 3. Photographic images of (a) a hydrogel and (b) a hydrogel containing double-helical Au NWs. (c, d) High- and low-magnification TEM images of double-helical Au NWs and (e) a twisted nanoribbon composed of C18AA and D-HSA. Scale bars: (c) 500 nm and (d, e) 100 nm.

To determine the helicities of the double-helical Au NWs, TEM tomography was conducted by acquiring TEM images of the Au NWs at various tilt angles. It is clear that Au NWs prepared from the D- and L-HSA systems have right- and left-handed helicities, respectively (Figure 4a–d), which cor-

respond to those of the twisted nanoribbons that served as the templates. Furthermore, dispersions of the right- and left-handed helical Au NWs exhibit opposite CD spectra; these spectra were clearly different to those of the twisted nanoribbons (Figure 4e). Weak CD signals in 300–350 nm region are derived from soft-templates with right- and left-handed twist. Thus, broad CD signals in 400–800 nm region originated from helical Au NWs. Further, the profiles and the signs of CD signals of right- and left-handed helical Au NWs dispersions were similar to recently reported results<sup>4k</sup> that obtained from helical stackings of anisotropic straight Au nanowire layers. Accordingly, chirality was successfully transcribed from the organic template to the Au nanocrystals by wet chemical synthesis.

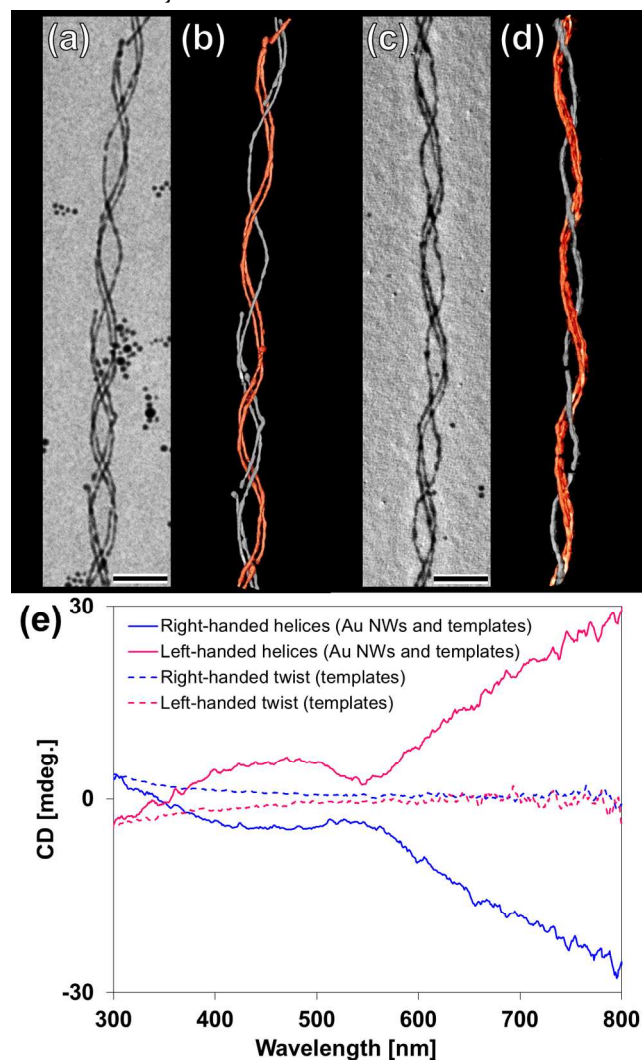


Figure 4. (a, c) TEM images and (b, d) the corresponding TEM-tomography images of Au NWs prepared from right- and left-handed templates, respectively. Scale: 50 nm. (e) CD spectra of dispersions of right- (blue solid line) and left-handed (red solid line) double-helical Au NWs with twisted nanoribbons and nanoribbons with right- (blue broken line) and left-handed twist (red broken line).

To investigate the mechanism for the formation of the double-helical Au NWs, high-resolution TEM images of the resultant Au NWs were acquired (Figure S18). A periodic fringe of 0.24 nm corresponding to the Au (111) lattice spacing, and multiple crystal grain boundaries were observed in the Au

NWs. Interestingly, relatively large single-crystalline domains were observed in the polycrystalline Au NWs. According to a previous report, the predominant growth in the (111) crystal direction is ascribed to C18AA preferring to cap the (100) and (110) crystal facets rather than the (111) facet.<sup>13</sup> Furthermore, the presence of crystal grain boundaries provides valuable information regarding the Au-NW growth process; i.e., Au NWs are probably produced by the gradual fusion of nanocrystals on the twisted nanoribbon template formed during the early stages of reduction. This growth-process hypothesis is also supported by the presence of Au NPs and short Au NWs on the edges of the templates during the early reduction period (Figure S19).

In summary, we introduced a wet chemical method for the synthesis of chirality-controlled double-helical Au NWs using twisted nanoribbon templates of HSA, which serves as the source of chirality, and C18AA, which acts as the Au capping agent. We demonstrated that the introduction of two compounds that individually perform different functions into the template is a highly effective method for the preparation of chiral Au nano-objects using wet chemistry. We believe that this bi-functional strategy can be applied to the synthesis of other shape-controlled metallic nano-objects.

## ASSOCIATED CONTENT

### Supporting Information

Experimental details and Supplementary Figures S1–S19. This material is available free of charge via the Internet at <http://pubs.acs.org>.

## AUTHOR INFORMATION

### Corresponding Author

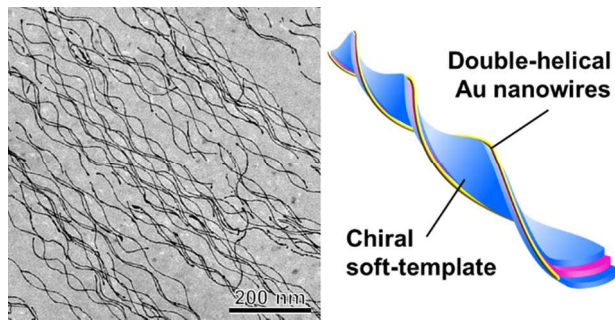
\*E-mail: [kawai@ci.kagu.tus.ac.jp](mailto:kawai@ci.kagu.tus.ac.jp)

### Notes

The authors declare no competing financial interests.

## REFERENCES

- (1) Liu, M.; Zhang, L.; Wang, T. *Chem. Rev.* **2015**, *115*, 7304–7397.
- (2) Zhang, M.; Qing, G.; Sun, T. *Chem. Soc. Rev.* **2012**, *41*, 1972–1984.
- (3) Soukoulis, C. M.; Wegener, M. *Nat. Photonics* **2011**, *5*, 523–530.
- (4) Pendry, J. B. *Science* **2004**, *306*, 1353–1355. (b) Zhang, S.; Park, Y.-S.; Li, J.; Lu, X.; Zhang, W.; Zhang, X. *Phys. Rev. Lett.* **2009**, *102*, 023901.
- (5) (a) Mark, A. G.; Gibbs, J. G.; Lee, T.-C.; Fischer, P. *Nat. Mater.* **2013**, *12*, 802–807. (b) Gibbs, J. G.; Mark, A. G.; Lee, T.-C.; Eslami, S.; Schamel, D.; Fischer, P. *Nanoscale* **2014**, *6*, 9457–9466. (c) Frank, B.; Yin, X.; Schäferling, M.; Zhao, J.; Hein, S. M.; Braun, P. V.; Giessen, H. *ACS Nano* **2013**, *7*, 6321–6329. (d) Yeom, B.; Zhang, H.; Zhang, H.; Park, J. I.; Kim, K.; Govorov, A. O.; Kotov, N. A. *Nano Lett.* **2013**, *13*, 5277–5283. (e) Esposito, M.; Tasco, V.; Todisco, F.; Cuscunà, M.; Benedetti, A.; Sanvitto, D.; Passaseo, A. *Nat. Commun.* **2015**, *6*, 6484. (f) Gansel, J. K.; Thiel, M.; Rill, M. S.; Decker, M.; Bade, K.; Saile, V.; von Freymann, G.; Linden, S.; Wegener, M. *Science* **2009**, *325*, 1513–1515. (g) Helgert, C.; Pshenay-Severin, E.; Falkner, M.; Menzel, C.; Rockstuhl, C.; Kley, E.-B.; Tünnermann, A.; Lederer, F.; Pertsch, T. *Nano Lett.* **2011**, *11*, 4400–4404. (h) Hentschel, M.; Schäferling, M.; Weiss, T.; Liu, N.; Giessen, H. *Nano Lett.* **2012**, *12*, 2542–2547. (i) Kim, Y.; Yeom, B.; Arteaga, O.; Yoo, S. J.; Lee, S.-G.; Kim, J.-G.; Kotov, N. A. *Nat. Mater.* **2016**, *15*, 461–468. (j) Toyoda, K.; Miyamoto, K.; Aoki, N.; Morita, R.; Omatsu, T. *Nano Lett.* **2012**, *12*, 3645–3649. (k) Lv, J.; Hou, K.; Ding, D.; Wang, D.; Han, B.; Gao, X.; Zhao, M.; Shi, L.; Guo, J.; Zheng, Y.; Zhang, X.; Lu, C.; Huang, L.; Huang, W.; Tang, Z. *Angew. Chem. Int. Ed.* **2017**, *56*, 5055–5060.
- (6) (a) Zhou, C.; Duan, X.; Liu, N. *Acc. Chem. Res.* **2017**, *50*, 2906–2914. (b) Sharma, J.; Chhabra, R.; Cheng, A.; Brownell, J.; Liu, Y.; Yan, H. *Science* **2009**, *323*, 112–116. (c) Wu, X.; Xu, L.; Ma, W.; Liu, L.; Kuang, H.; Kotov, N. A. *Adv. Mater.* **2016**, *28*, 5907–5915. (d) Shemer, G.; Krichevski, O.; Markovich, G.; Molotsky, T.; Lubitz, I.; Kotlyar, A. B. *J. Am. Chem. Soc.* **2006**, *128*, 11006–11007. (e) Yan, W.; Xu, L.; Xu, C.; Ma, W.; Kuang, H.; Wang, L.; Kotov, N. A. *J. Am. Chem. Soc.* **2012**, *134*, 15114–15121.
- (7) (a) Song, C.; Blaber, M. G.; Zhao, G.; Zhang, P.; Fry, H. C.; Schatz, G. C.; Rosi, N. L. *Nano Lett.* **2013**, *13*, 3256–3261. (b) Chen, C.-L.; Zhang, P.; Rosi, N. L. *J. Am. Chem. Soc.* **2008**, *130*, 13555–13557. (c) Chen, C.-L.; Rosi, N. L. *J. Am. Chem. Soc.* **2010**, *132*, 6902–6903. (d) Zhang, C.; Song, C.; Fry, H. C.; Rosi, N. L. *Chem.—Eur. J.* **2014**, *20*, 941–945. (e) Merg, A. D.; Slocik, J.; Blaber, M. G.; Schatz, G. C.; Naik, R.; Rosi, N. L. *Langmuir* **2015**, *31*, 9492–9501. (f) Merg, A. D.; Boatz, J. C.; Mandal, A.; Zhao, G.; Mokashi-Punekar, S.; Liu, C.; Wang, X.; Zhang, P.; van der Wel, P. C. A.; Rosi, N. L. *J. Am. Chem. Soc.* **2016**, *138*, 13655–13663. (g) Mokashi-Punekar, S.; Merg, A. D.; Rosi, N. L. *J. Am. Chem. Soc.* **2017**, *139*, 15043–15048.
- (8) (a) Jung, S. H.; Jeon, J.; Kim, H.; Jaworski, J.; Jung, J. H. *J. Am. Chem. Soc.* **2014**, *136*, 6446–6452. (b) Zhu, L.; Li, X.; Wu, S.; Nguyen, K. T.; Yan, H.; Ågren, H.; Zhao, Y. *J. Am. Chem. Soc.* **2013**, *135*, 9174–9180. (c) George, J.; Thomas, K. G. *J. Am. Chem. Soc.* **2010**, *132*, 2502–2503. (d) Guerrero-Martínez, A.; Auguie, B.; Alonso-Gómez, J. L.; Džolić, Z.; Gómez-Graña, S.; Žinić, M.; Cid, M. M.; Liz-Marzán, L. M. *Angew. Chem. Int. Ed.* **2011**, *50*, 5499–5503. (e) Jin, X.; Jiang, J.; Liu, M. *ACS Nano* **2016**, *10*, 11179–11186.
- (9) (a) Cheng, J.; Saux, G. L.; Gao, J.; Buffeteau, T.; Battie, Y.; Barois, P.; Ponsinet, V.; Delville, M.; Ersen, O.; Pouget, E.; Oda, R. *ACS Nano* **2017**, *11*, 3806–3818. (b) Tamoto, R.; Lecomte, S.; Si, S.; Moldovan, S.; Ersen, O.; Delville, M.-H.; Oda, R. *J. Phys. Chem. C* **2012**, *116*, 23143–23152. (c) Qi, H.; Shopsowitz, K. E.; Hamad, W. Y.; MacLachlan, M. J. *J. Am. Chem. Soc.* **2011**, *133*, 3728–3731.
- (10) (a) Xie, J.; Duan, Y.; Che, S. *Adv. Funct. Mater.* **2012**, *22*, 3784–3792. (b) Xie, J.; Che, S. *Chem.—Eur. J.* **2012**, *18*, 15954–15959.
- (11) (a) Maoz, B. M.; van der Weegen, R.; Fan, Z.; Govorov, A. O.; Ellestad, G.; Berova, N.; Meijer, E. W.; Markovich, G. *J. Am. Chem. Soc.* **2012**, *134*, 17807–17813. (b) Ben-Moshe, A.; Wolf, S. G.; Sadan, M. B.; Houben, L.; Fan, Z.; Govorov, A. O.; Markovich, G. *Nat. Commun.* **2014**, *5*, 4302.
- (12) (a) Tachibana, T.; Kambara, H. *J. Am. Chem. Soc.* **1965**, *87*, 3015–3016.
- (13) (a) Mallia, V. A.; Weiss, R. G. *J. Phys. Org. Chem.* **2014**, *27*, 310–315. (b) Murakami, S.; Satou, K.; Kijima, T.; Watanabe, M.; Izumi, T. *Eur. J. Lipid Sci. Technol.* **2011**, *113*, 450–458.
- (14) (a) Morita, C.; Tanuma, H.; Kawai, C.; Ito, Y.; Imura, Y.; Kawai, T. *Langmuir* **2013**, *29*, 1669–1675. (b) Imura, Y.; Maezawa, A.; Morita, C.; Kawai, T. *Langmuir* **2012**, *28*, 14998–15004. (c) Imura, Y.; Morita, C.; Endo, H.; Kondo, T.; Kawai, T. *Chem. Commun.* **2010**, *46*, 578–579.
- (15) Imura, Y.; Tsujimoto, K.; Morita, C.; Kawai, T. *Langmuir* **2014**, *30*, 5026–5030.
- (16) Tachibana, T.; Mori, T.; Hori, K. *Nature* **1979**, *278*, 13–19.



1  
2  
3  
4  
5  
6  
7  
8  
9  
10  
11  
12  
13  
14  
15  
16  
17  
18  
19  
20  
21  
22  
23  
24  
25  
26  
27  
28  
29  
30  
31  
32  
33  
34  
35  
36  
37  
38  
39  
40  
41  
42  
43  
44  
45  
46  
47  
48  
49  
50  
51  
52  
53  
54  
55  
56  
57  
58  
59  
60